Rigorous statistical thermodynamical model for lattice dynamics in alloys

A. M. Santos [*]

Universidade Estadual de Mato Grosso do Sul, Dourados, Mato Grosso do Sul, C.P. 351, 79804-97, Brazil

H. W. L. Alves

Departamento de Ciências Naturais, Universidade Federal de São João del Rei, C.P. 110, 36.301-160, São João del Rei, MG, Brazil

C. A. Ataide,[†] I. Guilhon,[‡] M. Marques,[§] and L. K. Teles[‖]

*Grupo de Materiais Semicondutores e Nanotecnologia (GMSN), Instituto Tecnológico de Aeronáutica (ITA),
12228-900 São José dos Campos/SP, Brazil*

We propose another approach to overcome the difficulties of previous *ab initio* methods used to study lattice dynamics in disordered systems, such as alloys. Group III nitrides and arsenides are used as prototypical systems to validate the developed methodology. The phonon behaviors of ternary alloys, for specific concentrations, are calculated with a methodology based on the *ab initio* calculations of dynamics of the respective nitrides' and arsenides' bulks. The generalized phonons' behavior of long wavelengths for ternary alloys were simulated employing the generalized quasichemical approximation method to account for the inherent statistical disorder of the system. The model describes the evolution of optical phonons to the Γ point as a function of molar fraction for zinc blende ternary alloys for III arsenides and III nitrides for any arbitrary compositions. We have found that the obtained results are in good agreement with experimental data taken from Raman and IR measurements available in the literature.

I. INTRODUCTION

From cell phones, computer chips, and solar cells, lattice vibrations play an essential role in understanding the transport of heat. In particular, phonons, quantized modes of vibration, are intimately responsible for thermal conductivity and heat capacity in semiconductors and insulators, being also related to the electronic transport [1,2]. Moreover, they are fundamental for phonon-mediated superconductivity [3] and the description of phonon-polariton light-matter interaction [4]. Thus, to understand these phenomena, theoretical computational models able to provide an accurate description of materials lattice dynamics, in general, are desirable.

On the other hand, the progress of electronics and optoelectronics demands more and more sophisticated systems. For example, for decades, a common feature in electronic and optoelectronic devices has been the application of semiconductors alloys [5–7]. The alloys are vital components as the active layers in optical devices operated in high temperature for visible/ultraviolet spectral range, and high-power electronics [8,9]. The high flexibility in the properties of alloys is

obtained changing their chemical composition, which allows, in principle, their properties to be tuned continuously between the values correspondent of the pure compounds. This fantastic flexibility has been used extensively in three-dimensional devices and, more recently, has also been shown to be very promising for two-dimensional ones [10–15]. Considering the microscopic description of these systems, the complexity comes from the coexistence of atoms of different sizes on the crystalline lattice. A proper description of the oscillating system must consider a disordered distribution of masses and its influence on elastic interactions, leading to novel features in the phonon spectra. As examples, there are the resonance modes and splitting of the dispersion branches, and also modifications of both the vibrational eigenfrequencies and eigenvectors of the normal modes. It is also observed that the long-wavelength optical phonon in semiconductor alloys exhibits behaviors that are classed into two main classes denominated one or two mode. In the one-mode class, the frequencies vary continuously and approximately linearly with the molar fraction x of the alloy. In the case of the two-mode behavior, the two sets of optical modes correspond nearly to that of the two end components of the alloy [16].

From the theoretical point of view, the difficulties are twofold, namely (i) reproduction of an infinite disordered system and (ii) accurate description of lattice dynamics of such an inhomogeneous system. An approach to such systems, which has been widely used, is to consider semiempirical models and a quasirandom distribution of atoms, e.g., the modified

---

[*]adrianosnts2@gmail.com
[†]ataidecaa@gmail.com
[‡]guilhon@ita.br
[§]mmarques@ita.br
[‖]lkteles@ita.br

random element isodisplacement (MREI) method of Chang and Mitra [17], a generalization of the MRE [18]. Recently, more rigorous *ab initio* approaches based on density functional theory (DFT) [19,20] have been explored to describe oscillating systems by considering the linear-response [21] or the frozen-phonon [22] approaches. For instance, Wang *et al.* calculate the dynamical matrix, concerning the wave vector space of the ideal lattice, by averaging over the force constants of a special quasirandom structure (SQS) in the case of Cu_3Au, FePd, and NiPd alloys [23]. Also, with the itinerant coherent potential approximation (ICPA), SQS may be used to describe random alloys considering both mass and force-constant disorder [24,25]. Although SQS describes the alloy disorder, it is limited to specific concentrations. Another kind of approach is to use virtual crystal approximation (VCA) to simulate the alloys, as in the work of Murphy and Fahy to obtain carrier-phonon scattering in alloys spectrum in SiGe alloys [26]. De la Pena *et al.* used VCA to simulate electron-phonon interaction and superconductivity in Tl-Pb-Bi alloys [27]. Although with VCA any composition of the alloy can be simulated, the description of the disorder neglects the environmental effects, such as composition fluctuation, in the local virtual average potential for atoms. Additionally, other methods try to include the effect of multisite random correlations as important features of the lattice dynamics problem [28,29]. In summary, the description of the lattice dynamics has been significantly improved, while the disorder description is still attached to quasirandom atomic distributions, disregarding any influence of energetics on local atomic arrangements. The absence of rigorous calculations contemplating, in equal footing, both aspects may be justified by the fact that the next level of description is the cluster expansion, which has a higher computational cost.

In this work, we propose an *ab initio* approach to address the complexity of the vibrational properties of alloys beyond previously proposed models. As a progress of the methodological development, we provide not only the state of art description of the lattice dynamics currently used, but mainly a more accurate description of the system disorder and its consequences on the vibrational properties. A cluster expansion, so-called generalized quasichemical approximation (GQCA) [5,10,11,13,14], is combined with calculations of total energy and phonon spectra within the DFT framework to include disorder and composition fluctuation effects. The disordered distribution of masses obtained from the statistical approach is considered, while approximations on the force constants and born effective charges are considered for intermediate molar fractions to avoid the high computational cost associated with the application of frozen-phonon calculation on a broad set of nonsymmetric clusters. As a benchmark, we consider the well established III-V nitride and arsenide alloys to validate our model. The presented approach is, however, general and can be applied in several different systems.

In Sec. II, we introduce the GQCA model and lattice dynamics methods. In Sec. III, we present our results for the vibrational density of states, zone-center optical phonon frequencies at the whole composition range for each semiconductor alloy. Our results are compared with experimental data whenever possible. Finally, in Sec. IV, a summary is given.

II. METHODOLOGY

A. Lattice dynamics

The potential energy of a periodic system can be written as a Taylor expansion in terms of the atomic displacements around the minimum-energy positions. Retaining only terms up to the quadratic order in the displacements, i.e., harmonic approximation, and considering that the allowed values of the wave vectors are chosen according to the Born–von Karman periodic boundary conditions, the vibrational properties are calculated by solving the following matrix equation:

$$(D - I\omega^2)W = 0, \tag{1}$$

where W is the polarization vector, ω is the phonon frequency, and D is the dynamical matrix [30–32]. Each element of the dynamic matrix is given as

$$D_{ij}^{KK'}(\vec{q}) = \sum_{l'} \frac{\Phi_{ij}^o(lK, l'K')e^{i\vec{q}\cdot[\vec{R}(l'K') - \vec{R}(lK)]}}{\sqrt{M_K M_{K'}}}, \tag{2}$$

where $\vec{R}(lK)$ presents the position of the atom K inside cell l, $\vec{q}$ is the wave vector, M_K is the mass of the K atom, i and j are Cartesian coordinates, and Φ is the atomic force constants tensor. This tensor is then calculated by

$$\Phi_{ij}^o(lK, l'K') = \frac{\partial F_j(l'K')}{\partial u_i(lK)}, \tag{3}$$

where $\vec{u}(lK)$ is the atomic displacement of lK atom and $\vec{F}(lK)$ are the forces on atoms with a finite displacement.

For perfect covalent materials, the optical branches LO and TO are degenerate at the Γ point, while there is a breakdown of this degeneracy for the ionic ones. As the long-range dipole-dipole interaction of the LO mode breaks the periodic boundary condition, the harmonic approximation is not enough to treat this phonon branch. A nonanalytical term can be added to the dynamical matrix, to overcome this limitation, as follows [21,32–34]:

$$D_{ij}^{KK'}(\vec{q} \to 0) = D_{ij}^{KK'}(\vec{q} = 0)$$
$$+ \frac{4\pi \left[\sum_k q_k Z_{ki}^K \right] \left[\sum_{k'} q'_k Z_{k'j}^K \right]}{\Omega_o \sqrt{M_K M'_K} \sum_{ij} q_i \epsilon_{ij}^\infty q_j}, \tag{4}$$

where $Z_{k'j}^K$ is the Born effective charge tensor of the K atom, Ω_o is the volume of the unit cell, and ϵ_{ij}^∞ is the high frequency dielectric constant tensor.

In this work, the force constants with respective Born effective charges are calculated by a direct approach, which requires the use of large supercells. This approach can be implemented for a single periodic system. However, its application for a disordered or quasidisordered system such as alloys is not straightforward.

B. Statistical approach for alloys

Since alloys are complex systems whose physical properties may be influenced by disorder effects, composition fluctuations, and phase separations, their investigation by *ab initio* methods is a great challenge and requires the use of proper approximations.

In this work, we apply the generalized quasichemical approximation to investigate such systems performing a cluster expansion of $A_x B_{1-x} C$ pseudoternary zinc blende alloys. The disordered systems are modeled as an ensemble of statistical and energetically independent cluster classes [5,35,36].

As further described elsewhere [5,10,13], the occurrence probability x_j of each cluster class j is determined by the minimization of the Helmholtz free energy, respecting the following constraints of normalization of total probability and average composition

$$\sum_{j=0}^{J} n_j x_j = nx, \qquad (5)$$

where n_j is the number of A atoms per cluster class j.

The probability x_j of a random cluster belonging to class j is given by the expression

$$x_j = \frac{g_j \lambda^{n_j} e^{-\varepsilon_j / k_B T}}{\sum_{j=0}^{J} g_j \lambda^{n_j} e^{-\varepsilon_j / k_B T}}, \qquad (6)$$

where g_j is the cluster symmetry degeneracy, ε_j is total energy per cluster j, and λ is a positive constant determined by the application of the average composition constraint expressed in Eq. (5).

An arbitrary physical property can be estimated as a statistical average $p(x, T)$ of quantities p_j calculated for each cluster class j, weighted by the occurrence probability distribution $x_j(x, T)$, i.e.,

$$p(x, T) = \sum_{j=0}^{J} x_j(x, T) p_j. \qquad (7)$$

In the present work, we focus our attention on frequencies ω_{LO} and ω_{TO}, respectively associated with LO or TO modes of Γ phonons.

Composition fluctuation effects can be estimated by considering mean-squared deviations around the average value

$$\Delta p(x, T) = \sqrt{\sum_{j=0}^{J} x_j p_j^2 - \left(\sum_{j=0}^{J} x_j p_j \right)^2}. \qquad (8)$$

Total energies ε_j and physical properties p_j of each nonequivalent cluster class are calculated within the density functional theory (DFT) framework, as implemented in the VASP code [37]. Further computational details are provided in Sec. II D.

Finally, we emphasize that the implementation of the GQCA method to describe the disordered quasidisordered distribution of atoms in alloyed systems requires the simulation of each possible atomic arrangement of a previously defined cluster. The number of atoms of each cluster must be determined between the limits of a (i) small size leading to a small number of configurations (low computational cost) but poor disorder description and (ii) a very large size with large number of configurations (high computational cost) and a very rich description of alloy disorder. In this work, we consider supercells with 16 atoms for the cluster expansion of the alloyed systems.
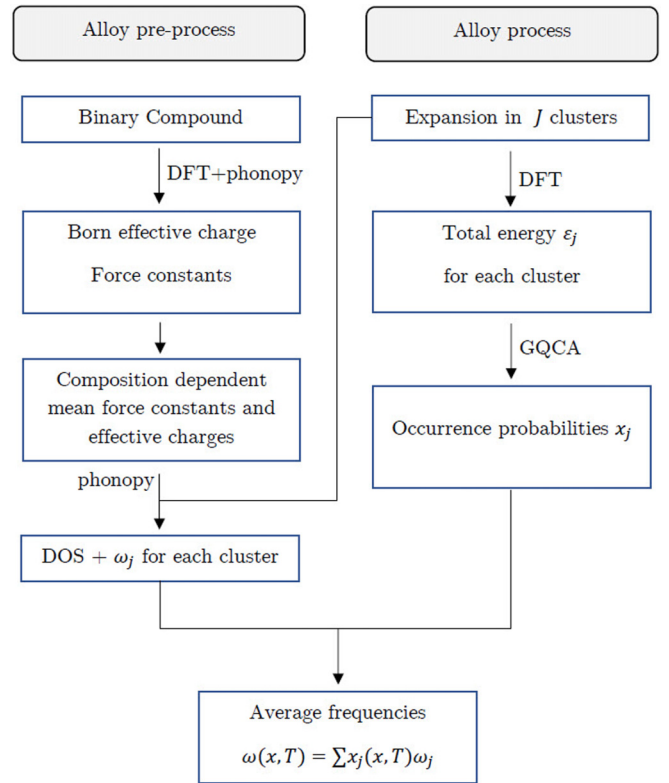
FIG. 1. Workflow of proposed statistical model for lattice dynamics in alloys. The alloy preprocess covers the calculation of composition dependent mean force constants and born effective charges, while the alloy process covers the cluster expansion of the system in clusters and the calculation of average frequencies.

C. Statistical approach for lattice dynamic in alloys

In order to simulate the lattice dynamics of an alloy, we have to deal with two conflicting demands: a large supercell for the calculation of lattice dynamics and the related increasing number of cluster configurations. This challenge is accomplished by considering reasonable approximations. Due to the large supercell size that would be required to simulate the vibrational properties of the ternary alloys for each 16-atom cluster of each class, the adopted methodology was to use the binaries' alloy *ab initio* results to define the specific set of parameters values that characterized each related ternary alloy molar concentration. In this way, assuming a linear behavior for both force constant tensor and ionic parameters, we have determined the short- and long-range interaction for each ternary alloy concentration, making possible, for each ternary alloy, the calculation of phonon frequencies ($\omega_j^{LO,TO}$) for each average concentration x and configuration j.

Since it is not possible to evaluate the LO and TO phonon frequencies at the concentration extrema with a 16-atoms cluster, we considered a 128-atom supercell to identify the vibrational LO and TO modes of a substitutional "impurity" atom for very low compositions.

In order to provide an overview of the proposed *ab initio* statistical approach for lattice dynamics, we provide the workflow illustrated in Fig. 1. Mean force constants and born effective charges are determined in the so-called "alloy

preprocess." The average phonon frequencies $\omega(x, T)$ of optical modes in Γ are calculated from distribution of the occurrence probabilities $x_j(x, T)$ and application of mean force constants and effective charge on each nonequivalent cluster class obtained in the cluster expansion of an alloyed system, which we named "alloy process."

Then, we evaluated the Born effective charges and the dielectric tensor, which is a necessary parameter to obtain the full phonon behavior for binary crystals.

To provide a good description of short and long-range interactions, we have used a supercell with 128 atoms to *ab initio* calculations of vibrational behavior for binary crystals.

Finally, the presented statistical framework for the description of lattice dynamic in alloys makes use of the disordered distribution of masses determined by GQCA avoiding the substantial computational costs associated with the calculation of force constant tensors for each cluster class considered by the GQCA formalism by considering weighted force constants and Born effective charges between the alloy end components.

D. Computational details

In order to feed the presented statistical model, total energies ε_j and physical properties p_j of each nonequivalent cluster class are calculated within the density functional theory (DFT) framework as implemented in Vienna *Ab Initio* Simulation Package (VASP) [37]. We have employed local density approximation (LDA) to the exchange-correlation energy functional as proposed by Ceperly and Alder parametrized by Perdew and Zunger in total energy calculations [38,39]. Kohn-Sham equations were solved in the projector augmented wave method (PAW) [40]. We have used an energy cutoff parameter of $E_{cut} = 600$ eV and a $40 \times 40 \times 40$, $10 \times 10 \times 10$, and $1 \times 1 \times 1$ Γ-centered k-point mesh in the Monkhorst-Pack scheme for cells with, respectively, 2, 16, and 128 atoms. The total energy convergence for all electronic steps was set at 10^{-8} eV. All atomic coordinates were relaxed until the Hellmann-Feynman forces were small in proportion to the convergence in energy, using the criterion that the energy difference between two successive changes of atomic positions was lower than 10^{-7} eV. For each binary compound, the force constant tensor and Born effective charges are determined considering harmonic approximation as implemented in PHONOPY [32].

We considered 16-atom clusters, whose $n = 8$ cation sites are occupied by all possible combinations of A and B. The $2^8 = 256$ possible atomic arrangements are organized into $J = 16$ nonequivalent cluster classes with different degeneracies g_j by considering the T_d space group symmetry operations.

III. RESULTS AND DISCUSSIONS

Figure 2 depicts the results for the phonon density of states (DOS) of 16 nonequivalent clusters describing the zinc blende AlGaAs (a), AlInAs (b), and InGaAs (c), represented by the continuous lines. From Figs. 2(a) and 2(b), one observes that the phonon two-mode behavior is evident by the separation
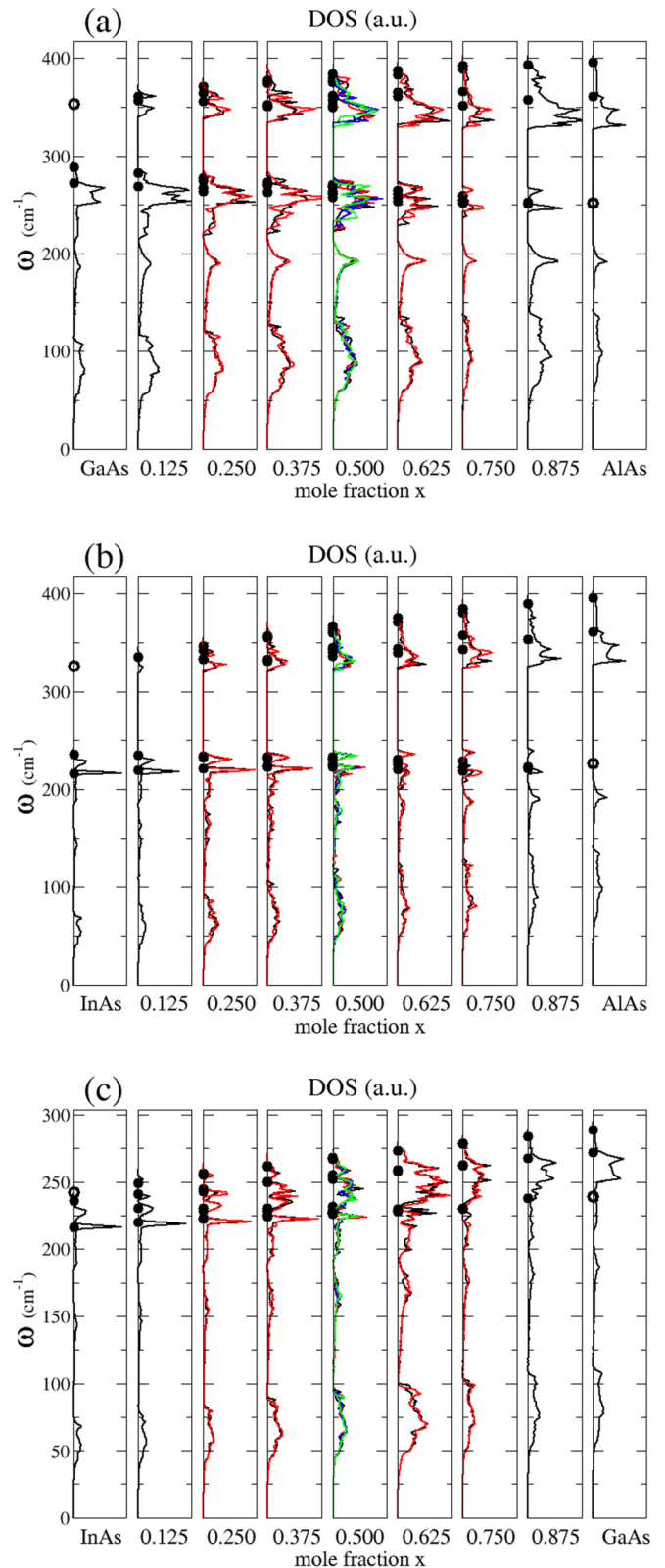
FIG. 2. Evaluated phonon density of states dependence with the alloy concentration for cubic (a) AlGaAs, (b) AlInAs, and (c) InGaAs alloys. When there is more than one cluster class for a given molar fraction, the DOS curves are distinguished by black, red, blue, and green colors. The black circles represent the frequencies of the zone centered phonons for each cluster, while open circles are derived from vibrational optical modes for substitutional impurities.

of the optical branches as the Al concentration increases. At low concentrations, there is the appearance of vibrational modes assigned to AlAs modes in the region above the GaAs(InAs) optical branches. For high Al concentrations, vibrational modes assigned to GaAs (InAs) appear in the AlAs frequency gap between the acoustical and optical branches. For the evaluated InGaAs DOS, we have detected a separation of the optical branches for low concentrations, indicating a two-mode phonon behavior. However, as the Ga concentration increases, this separation did not become evident as in previous cases.

The black circles in Fig. 2 are drawn for a guide to the eyes for the correct LO ant TO phonon assignment in the long wavelength region, which was obtained by an analysis of the vibrational modes of each cluster configuration j. The two-mode behavior observed in our evaluated DOS for AlGaAs alloys are in agreement with other *ab initio* results [41]. However, for InGaAs, they contradict the calculated DOS by using molecular dynamics [42], which does not show the optical branches separation. The substitutional "impurity" LO and TO vibrational modes at composition extrema with 128-atom supercells are assigned by the open circles drawn in Fig. 2.

Once the phonon modes and their frequencies are determined for each cluster, the GQCA method evaluates the frequencies of zone-center phonons versus composition for each branch. We display our obtained zone center modes compared with the experimental data [42–46] in Fig. 3. The agreement is very good. Our calculations of the phonon energies clearly indicate a two-mode behavior for all arsenide alloys studied. The results show a relationship between the inclination of the TO phonons and the intensity of the parameters related to the short-range interactions. A quantitative similarity, within 1%, between the constant force tensors of AlAs and GaAs binaries is verified. InAs exhibits the same qualitative behavior, but reduced force constants about 15%, when compared with the previous compounds. The difference between the calculated parameters that characterize the extremes of the AlInAs and InGaAs alloys causes the TO phonons to have a rising slope with In concentration when compared to the TO phonons behavior of the AlGaAs.

For In concentration higher than 80% in InGaAs alloys, no significant difference of frequency is observed between LO1 and TO1 optical modes, which is consistent with reported experimental findings [47].

The same procedure was employed to simulate the vibrational DOS that was applied to cubic III nitrides. The obtained results for the vibrational DOS of AlGaN, AlInN, and InGaN are displayed in Fig. 4. As in the previous cases, the black circles represent the frequencies of the zone centered phonons for each cluster, while open circles are derived from vibrational optical modes for substitutional impurities. Different from AlGaAs and AlInAs, where the continuous two-phonon mode behavior is evident from Fig. 2, it is possible to observe that for low concentrations there is an unfolding associated to the vibrational mode of the AlN in the region immediately above the optical branches of both GaN and InN, indicating an apparent two-mode behavior in AlGaN and AlInN, as
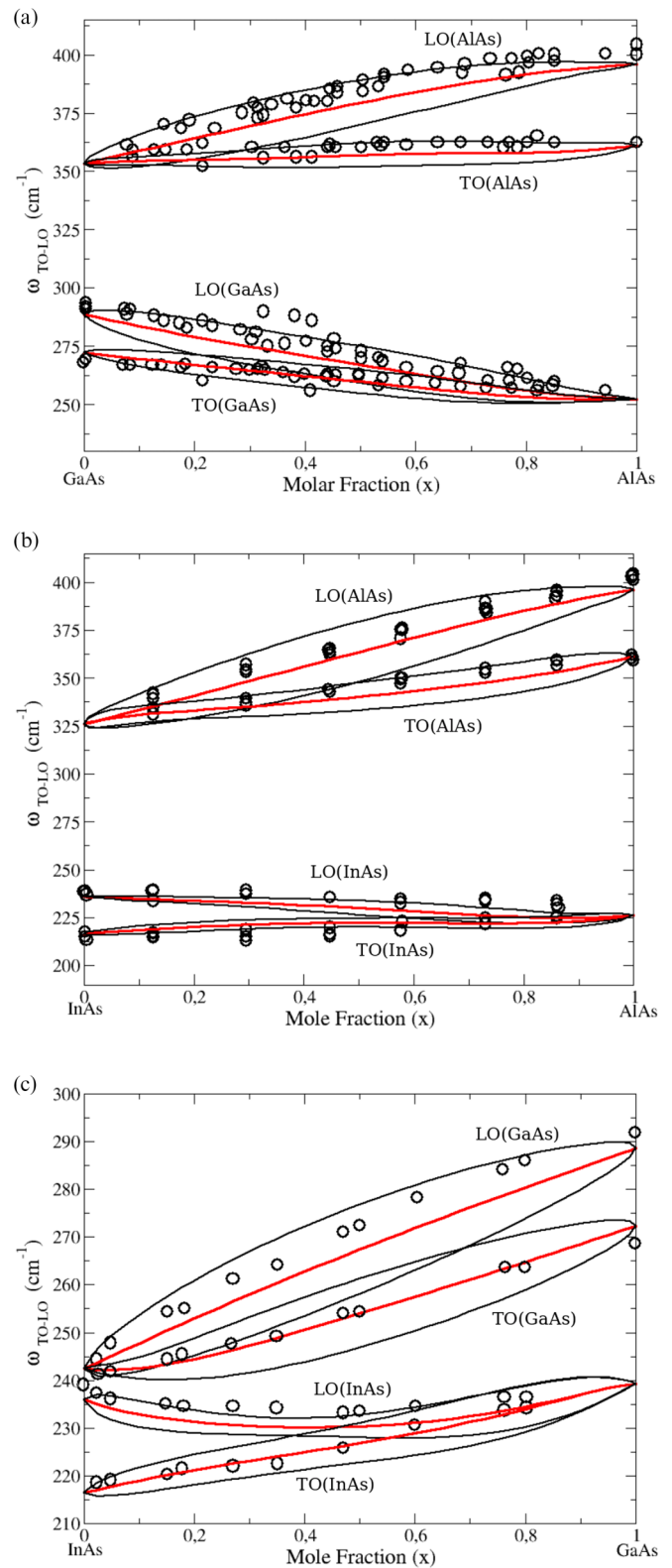
FIG. 3. Evaluated zone-center phonon frequencies dependence with mole fraction x and respective mean-square deviations for (a) AlGaAs, (b) AlInAs, and (c) InGaAs, represented in red and black solid lines, respectively. Available experimental data [42–46] is depicted by open circles for comparison.
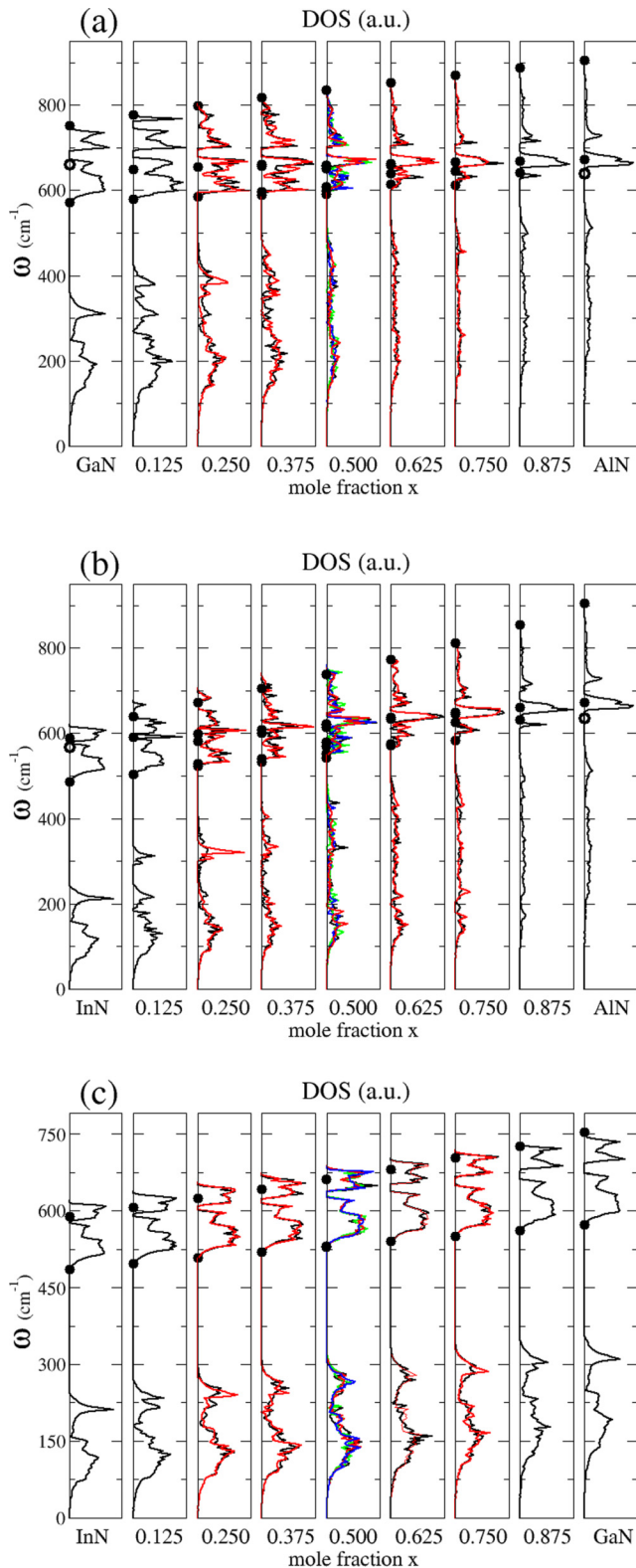
FIG. 4. Evaluated phonon density of states dependence with the alloy concentration for cubic (a) AlGaN, (b) AlInN, and (c) InGaN alloys. When there is more than one cluster class for a given molar fraction, the DOS curves are distinguished by black, red, blue, and green colors. The black circles represent the frequencies of the zone centered phonons for each cluster, while open circles are derived from vibrational optical modes for substitutional impurities.

depicted in Fig. 4. However, there is no perceptible unfolding in this same region for the other concentrations.

Unlike from the AlN case, where the contribution of the Al and N atoms is observed in optical and acoustic branches, the mass difference between Ga and N in GaN causes Ga to have a strong vibrational contribution in the region of the acoustic branches, while the N in the region of the optical branches. The same vibrational behavior occurs in InN. Therefore, the one-mode behavior in InGaN can be explained by the similarity and the high contribution of N to the optical vibrational modes in both GaN and InN.

As observed in arsenides, the force constant tensor of AlN and GaN exhibits variations about 5%, while InN exhibits reduced force constants about 20% smaller than the previous compounds. Additionally, previous works reported a weak dependence of the averaged bond lengths with respect to composition [5], indicating weak influence of the environment on the force constants. We do not expect differences between the actual force constants and the ones considered in our model significantly larger than 5% for any of the considered compounds.

We compare the obtained zone-center phonon frequency results with the available experimental data [48–51] in Fig. 5. The overall agreement by the proposed statistical approach is excellent. Our results show that while InGaN phonons behave as one mode, AlGaN and AlInN show a phonon one mode type to the LO branch and a two mode for TO branch.

The structural similarity for atom neighborhood and a strong dependence of the vibrational dynamics with the short-range interactions indicate that the zinc blende and wurtzite structures must present similar behaviors for the phonon modes.

The direct application of the MREI shows the one mode behavior for all cubic nitride alloys [30,48], but the experimental results for wurtzite AlGaN and some cubic AlGaN indicate the presence of the two-mode behavior [50,52,53], while experimental results for cubic and wurtzite InGaN conduct to the same one mode behavior [51,54,55]. Simulations performed by Grille *et al.* [16], using generalized MREI to describe the phonons for long wavelength, show close results to the considered nitrides.

Up to our knowledge, there is no experimental data for AlInN in the cubic structure. Thus we compare our results with experimental results for the wurtzite phase [56,57]. The agreement with experiment is satisfactory.

Finally, we provide adjusted fitting parameters for each zone-center phonon optical mode considering the expression $\omega(x) = b(1 - x)x + \omega_1 x + \omega_0(1 - x)$ shown in Figs. 3 and 5. The bowing parameter is given by b, while ω_0 and ω_1 provide the phonon frequencies for mole fractions $x = 0$ and $x = 1$, respectively. The results are listed in Table I. Considering the magnitude of zone-center frequencies for the end compounds and fitted bowing parameters obtained within GQCA that many optical branches can be satisfactorily described by a linear behavior, while others, e.g., LO(InAs) mode in InGaAs, present very significant bowing parameters. The obtained results are in agreement with experimental data available in literature [48].
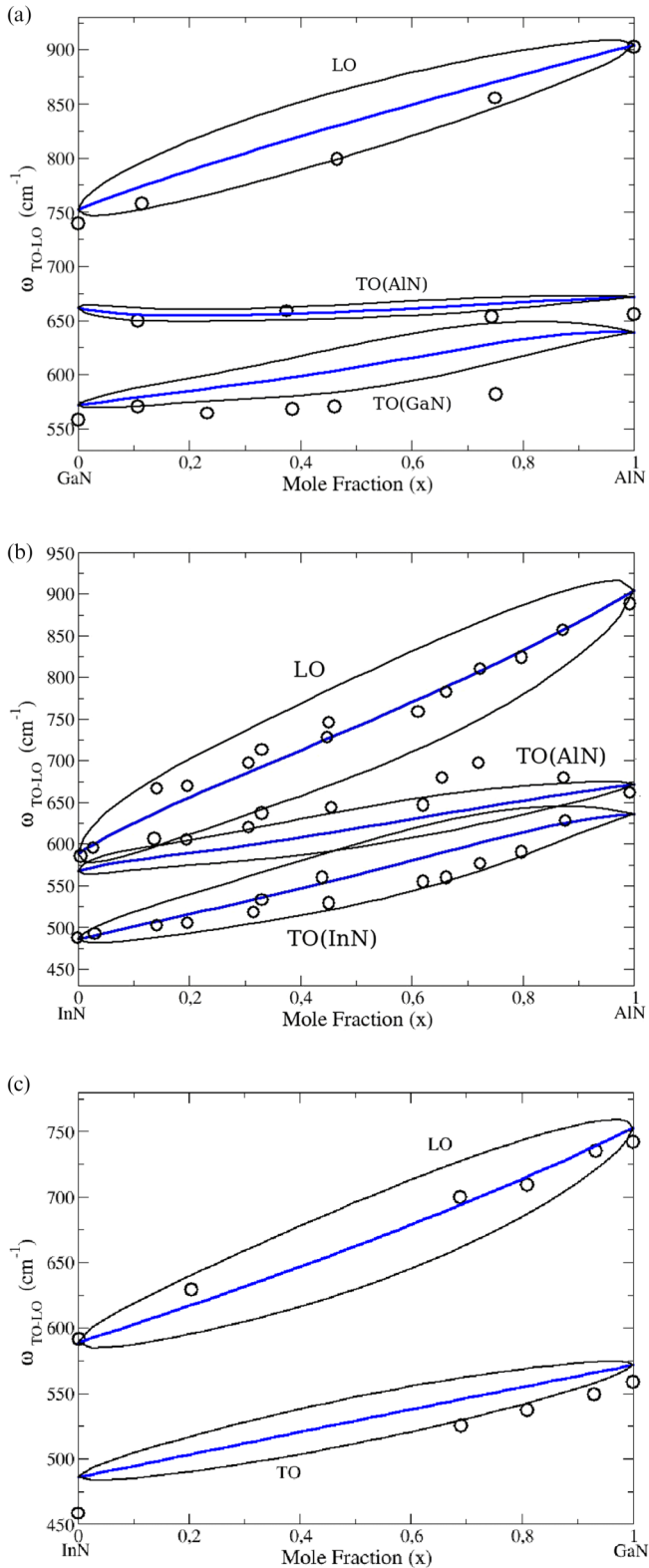
FIG. 5. Evaluated zone-center phonon frequencies dependence with mole fraction x and respective mean-square deviations for (a) AlGaN, (b) AlInN, and (c) InGaN, represented in blue and black solid lines, respectively. Available experimental data [48–51] is depicted by open circles for comparison.

TABLE I. Fitted parameters $\omega(x) = b(1-x)x + \omega_1 x + \omega_0(1-x)$ for the zone-center frequencies for each phonon optical mode.

		b (cm^{-1})	ω_1 (cm^{-1})	ω_0 (cm^{-1})
AlGaAs	TO(GaAs)	−11.2	272.3	252.3
	LO(GaAs)	−15.3	288.6	252.3
	TO(AlAs)	−2.5	353.3	361.2
	LO(AlAs)	19.3	353.3	396.1
AlInAs	TO(InAs)	1.9	216.5	226.2
	LO(InAs)	−6.0	235.9	226.2
	TO(AlAs)	−12.5	326.0	361.2
	LO(AlAs)	10.7	326.0	396.1
InGaAs	TO(InAs)	−3.1	239.3	216.5
	LO(InAs)	−28.9	239.3	235.9
	TO(GaAs)	−15.0	272.3	242.5
	LO(GaAs)	7.4	288.6	242.5
AlGaN	TO(GaN)	11.8	571.8	639.2
	TO(AlN)	−34.8	661.5	672.1
	LO	26.0	752.7	904.5
AlInN	TO(InN)	16.8	486.0	635.6
	TO(AlN)	−0.8	568.0	672.1
	LO	−19.0	588.9	904.4
InGaN	TO	1.0	571.8	486.0
	LO	−33.6	752.7	589.0

IV. SUMMARY AND CONCLUSIONS

In summary, we present an accurate and efficient methodology based on the *ab initio* parameters for short- and long-range interaction of group III of cubic binary nitrides and arsenides to calculate the vibrational properties of the respective cubic ternary alloys.

To treat the dispersion of long-wavelength phonon frequencies for each respective concentration, a statistical analysis within the GQCA method was used. Phonon frequencies, vibrational modes, and density of states were calculated from a 16 atom supercell by using a linear variation of the *ab initio* force constants with composition, followed by diagonalization of the dynamical matrix. This assumption is not essential to the GQCA application on vibrational properties of alloyed systems, but a simplifying hypothesis to perform the systematic cluster expansion of the system avoiding prohibitive computational costs. The theoretical model can be easily adapted to consider the nonlinear variations of force constants with composition.

The results for vibrational DOS for AlGaAs and AlInAs show a two-mode behavior. An analysis of the vibrational modes for the Γ point shows that the InGaAs also exhibits two-mode behavior, but with a narrowing of the TO and LO modes, associated with the InN, that occurs with the increasing Ga concentration. The same analysis shows a one-mode behavior for InGaN, while the AlGaN and InGaN present a two-mode behavior only for TO, where it is observed that the TO(AlN) phonon is located in a region of high concentration for the state density.

The results are in agreement with the experimental data, showing that the framework here presented is adequate and can assist theorists in further phonon studies on novel materials.

ACKNOWLEDGMENTS

[1] E. Pop, S. Sinha, and K. E. Goodson, Proc. IEEE **94**, 1587 (2006).

[2] P. G. Le Comber and W. E. Spear, Phys. Rev. Lett. **25**, 509 (1970).

[3] X. Wan, H.-C. Ding, S. Y. Savrasov, and C.-G. Duan, Phys. Rev. B **87**, 115124 (2013).

[4] K. C. Huang, P. Bienstman, J. D. Joannopoulos, K. A. Nelson, and S. Fan, Phys. Rev. B **68**, 075209 (2003).

[5] L. K. Teles, J. Furthmüller, L. M. R. Scolfaro, J. R. Leite, and F. Bechstedt, Phys. Rev. B **62**, 2475 (2000).

[6] J. Batey and S. L. Wright, J. Appl. Phys. **59**, 200 (1986).

[7] S. Wirths, R. Geiger, N. von den Driesch, G. Mussler, T. Stoica, S. Mantl, Z. Ikonic, M. Luysberg, S. Chiussi, J. M. Hartmann, H. Sigg, J. Faist, D. Buca, and D. Grützmacher, Nat. Photon. **9**, 88 (2014).

[8] J. G. Cody, D. L. Mathine, R. Droopad, G. N. Maracas, R. Rajesh, and R. W. Carpenter, J. Vac. Sci. Technol. B **12**, 1075 (1994).

[9] L. Shen, S. Heikman, B. Moran, R. Coffie, N.-Q. Zhang, D. Buttari, I. P. Smorchkova, S. Keller, S. P. DenBaars, and U. K. Mishra, IEEE Electron Device Lett. **22**, 457 (2001).

[10] I. Guilhon, L. K. Teles, M. Marques, R. R. Pela, and F. Bechstedt, Phys. Rev. B **92**, 075435 (2015).

[11] I. Guilhon, M. Marques, L. K. Teles, and F. Bechstedt, Phys. Rev. B **95**, 035407 (2017).

[12] M. Petrović, M. H. von Hoegen, and F.-J. M. zu Heringdorf, Appl. Surf. Sci. **455**, 1086 (2018).

[13] I. Guilhon, F. Bechstedt, S. Botti, M. Marques, and L. K. Teles, Phys. Rev. B **95**, 245427 (2017).

[14] I. Guilhon, F. Bechstedt, S. Botti, M. Marques, and L. K. Teles, J. Phys. Chem. C **121**, 27603 (2017).

[15] N. Morimoto, T. Kubo, and Y. Nishina, Sci. Rep. **6**, 21715 (2016).

[16] H. Grille, C. Schnittler, and F. Bechstedt, Phys. Rev. B **61**, 6091 (2000).

[17] I. F. Chang and S. S. Mitra, Phys. Rev. **172**, 924 (1968).

[18] Y. S. Chen, W. Shockley, and G. L. Pearson, Phys. Rev. **151**, 648 (1966).

[19] P. Hohenberg and W. Kohn, Phys. Rev. **136**, B864 (1964).

[20] W. Kohn and L. J. Sham, Phys. Rev. **140**, A1133 (1965).

[21] P. Giannozzi, S. de Gironcoli, P. Pavone, and S. Baroni, Phys. Rev. B **43**, 7231 (1991).

[22] S. Wei and M. Y. Chou, Phys. Rev. Lett. **69**, 2799 (1992).

[23] Y. Wang, C. L. Zacherl, S. Shang, L.-Q. Chen, and Z.-K. Liu, J. Phys.: Condens. Matter **23**, 485403 (2011).

[24] S. Ghosh, P. L. Leath, and M. H. Cohen, Phys. Rev. B **66**, 214206 (2002).

[25] O. Grånäs, B. Dutta, S. Ghosh, and B. Sanyal, J. Phys.: Condens. Matter **24**, 015402 (2011).

[26] F. Murphy-Armando and S. Fahy, Phys. Rev. B **78**, 035202 (2008).

[27] O. De la Peña-Seaman, R. Heid, and K.-P. Bohnen, Phys. Rev. B **86**, 184507 (2012).

[28] D. A. Biava, S. Ghosh, D. D. Johnson, W. A. Shelton, and A. V. Smirnov, Phys. Rev. B **72**, 113105 (2005).

[29] J. Kangsabanik, R. K. Chouhan, D. D. Johnson, and A. Alam, Phys. Rev. B **96**, 100201(R) (2017).

[30] G. P. Srivastava, *The Physics of Phonons* (CRC Press, Boca Raton, FL, 1990).

[31] P. Pavone, J. Phys.: Condens. Matter **13**, 7593 (2001).

[32] A. Togo and I. Tanaka, Scr. Mater. **108**, 1 (2015).

[33] R. M. Pick, M. H. Cohen, and R. M. Martin, Phys. Rev. B **1**, 910 (1970).

[34] X. Gonze and C. Lee, Phys. Rev. B **55**, 10355 (1997).

[35] C. Caetano, R. R. Pela, S. Martini, M. Marques, and L. K. Teles, J. Magn. Magn. Mater. **405**, 274 (2016).

[36] J. Ibáñez, S. Hernández, E. Alarcón-Lladó, R. Cuscó, L. Artús, S. Novikov, C. Foxon, and E. Calleja, J. Appl. Phys. **104**, 033544 (2008).

[37] G. Kresse and J. Furthmüller, Comput. Mater. Sci. **6**, 15 (1996).

[38] D. M. Ceperley and B. J. Alder, Phys. Rev. Lett. **45**, 566 (1980).

[39] J. P. Perdew and A. Zunger, Phys. Rev. B **23**, 5048 (1981).

[40] G. Kresse and D. Joubert, Phys. Rev. B **59**, 1758 (1999).

[41] M. Sternik, P. T. Jochym, and K. Parlinski, Comput. Mater. Sci. **13**, 232 (1999).

[42] P. S. Branicio, R. K. Kalia, A. Nakano, J. P. Rino, F. Shimojo, and P. Vashishta, Appl. Phys. Lett. **82**, 1057 (2003).

[43] D. J. Lockwood and Z. R. Wasilewski, Phys. Rev. B **70**, 155202 (2004).

[44] S. Adachi, *Properties of Aluminium Gallium Arsenide. No. 7* (IET, London, 1993).

[45] E. Sim, J. Beckers, S. De Leeuw, M. Thorpe, and M. A. Ratner, J. Chem. Phys. **122**, 174702 (2005).

[46] A. G. Milekhin, A. K. Kalagin, A. P. Vasilenko, A. I. Toropov, N. V. Surovtsev, and D. R. T. Zahn, J. Appl. Phys. **104**, 073516 (2008).

[47] E. J. Sim, M. W. Han, J. Beckers, and S. De Leeuw, Bull. Korean Chem. Soc. **30**, 857 (2009).

[48] S. Adachi, *Properties of Semiconductor Alloys: Group-IV, III-V and II-VI Semiconductors* (John Wiley & Sons, New York, 2009), Vol. 28.

[49] T. Frey, D. As, M. Bartels, A. Pawlis, K. Lischka, A. Tabata, J. Fernandez, M. Silva, J. Leite, C. Haug, and R. Brenn, J. Appl. Phys. **89**, 2631 (2001).

[50] H. Harima, T. Inoue, S. Nakashima, H. Okumura, Y. Ishida, S. Yoshida, T. Koizumi, H. Grille, and F. Bechstedt, Appl. Phys. Lett. **74**, 191 (1999).

[51] A. Tabata, J. Leite, A. Lima, E. Silveira, V. Lemos, T. Frey, D. As, D. Schikora, and K. Lischka, Appl. Phys. Lett. **75**, 1095 (1999).

[52] A. Cros, H. Angerer, O. Ambacher, M. Stutzmann, R. Höpler, and T. Metzger, Solid State Commun. **104**, 35 (1997).

[53] C. Wetzel and I. Akasaki, Emis Datarev. Ser. **23**, 143 (1999).

[54] M. Dutta, D. Alexson, L. Bergman, R. Nemanich, R. Dupuis, K. Kim, S. Komirenko, and M. Stroscio, Physica E **11**, 277 (2001).

[55] D. Alexson, L. Bergman, R. Nemanich, M. Dutta, M. Stroscio, C. Parker, S. Bedair, N. El-Masry, and F. Adar, J. Appl. Phys. **89**, 798 (2001).

[56] V. Naik, W. Weber, D. Uy, D. Haddad, R. Naik, Y. Danylyuk, M. Lukitsch, G. Auner, and L. Rimai, Appl. Phys. Lett. **79**, 2019 (2001).

[57] T. T. Kang, A. Hashimoto, and A. Yamamoto, Phys. Rev. B **79**, 033301 (2009).